American Journal of Civil Engineering and Architecture, 2018, Vol. 6, No. 5, 193-198
Available online at http://pubs.sciepub.com/ajcea/6/5/4
©Science and Education Publishing
DOI:10.12691/ajcea-6-5-4

Pull-out Resistance of Single Piles and Parametric Study using the Finite Difference Method (FDM)

Alex Otieno Owino[1,*], Zakaria Hossain[1], Jim Shiau[2]

[1]Department of Environmental Science Graduate School of Bioresources, Mie University, Japan
[2]Department of Civil Engineering and Surveying, University of Southern Queensland, Queensland, Australia
*Corresponding author: owinoalex55@gmail.com, 517M229@m.mie-u.ac.jp

Received August 12, 2018; Revised October 05, 2018; Accepted October 19, 2018

Abstract Many engineering structures both above ground and under the ground surface are subject to forces that create overturning moments upon them. In this study, the structure under consideration is the single pile foundation structure of solar panels. Increasing demand for clean energy is pushing for more economical means of constructing such structures with maximum evaluation focused on the cost of installation and the ultimate strength of the fully loaded structure hence single piles come into place. As studied in the previous paper on the design of the pile element, dimensions of *1.4m* pile foundation length and *0.26m* diameter are also employed in this paper to determine the pull-out capacity. Strength evaluation is done through numerical simulation using FLAC2D which use the finite difference method to evaluate the input codes in step by step manner while integrating the input parameters in a stress train relation as described in the pull-out code. The dimensions of the model mesh are twice the pile foundation depth, *2L* in the *y-direction* and *2L* in the *x-direction* from the pile vertical axis. Strength evaluation is done on sandy, clay and silty medium to determine the vast array of data for engineering design measures. A parametric study is then done by varying the foundation depth from *0.7m* to *2.0m*, soil angle of internal friction from 10^{o} to 40^{o} and the inclusivity of *gap* upon failure. The design dimensions show good bearing capacity with load up *to 94kN, 90kN* and *80kN* for dense sand, silty soil and clay soil respectively. The suggested relations for the pull-out capacity of the single pile regarding the axial ability are within design limits.

Keywords: *pull-out capacity, skin friction, finite difference method, stress-strain relation, FLAC2D*

Cite This Article: Alex Otieno Owino, Zakaria Hossain, and Jim Shiau, "Pull-out Resistance of Single Piles and Parametric Study using the Finite Difference Method (FDM)." *American Journal of Civil Engineering and Architecture*, vol. 6, no. 5 (2018): 193-198. doi: 10.12691/ajcea-6-5-4.

1. Introduction

Pile foundations are commonly used in support of engineering structures to prevent them from overturning moments produced by winds and earthquakes in most cases. To understand how piles, transmit the loads to the ground, several experiments are necessary before construction. In literature, the pull-out capacity of pile foundations has been carried out in a few studies most of which employ full-scale field experiments. In the previous research [1] it is suggested that static cone penetration test can be used in the estimation of the pile ultimate lifting capacity with the most determining factor being the uplift skin friction. The value obtained however needed some adjustments which led to the introduction of the reduction factor which was highly dependent on the soil type and the type of pile used in the construction and reduction values on the uplift load if the force was oscillating.

A large-scale experimental set up in [2] focused on the analysis of the pull-out loads. Their experiment was mainly based on fixed pile dimension installed in soft moist silty to fine clayey sand. The results obtained were used in the formulation of the equation: $Pu = \pi d\ L/2\ (KL \tan\theta + 2c)$ where K represented the coefficient of lateral earth pressure. However, their approach reflected the effect of type of casing and method of backfilling on the uplift capacity.

In accordance to the fact that the uplift capacity of the pile is dependent on the relative skin friction on the pile-soil interface, Sowa (1970), analysis on the field tests on cast piles depicted that the coefficient of the earth pressure was considerably less during loading than the ratio of earth pressure at rest and Rankine's active earth pressure coefficient. Due to this variation, it was perverse to set value during the preliminary design [3].

To counter the fluctuation of the earth pressure coefficient, Meyerhof [4], introduced the uplift coefficient in place of the factor of earth pressure. For a pile installed at an angle of shearing resistance θ, the uplift coefficient increased with the increase in the slenderness ratio L/d up to a maximum value, then remained constant. However, the limiting factor was shown to increase with an increase in angle of shearing resistance.

McClelland [5], demonstrated the effects of installation on the uplift capacity of piles by field tests on same steel pipe piles of diameter *508 mm* installed to penetration of

14.63m in uniform beach sand by four different techniques. The driven pile exhibited net uplift capacity, which was 1.4 times that of a pile installed by jetting with external return flow. He concluded that the ultimate shaft resistance was dependent on the methods of driving/installation.

More research in [6], suggested the evaluation of the ultimate loading capacity of the piles was by the assessment of the skin friction along the pile and soil interface and the bearing pressure along the perimeter of the pile. Using this proposed approach, the ultimate bearing capacity became a function of the diameter of the pile, d, depth of the center of the first under-reamed bulb, d_l, thickness of the center of the last under-reamed bulb, d_n, diameter of the under-reamed bulb, B_l, number of under-reamed bulb, n, coefficient of earth pressure and the bearing capacity depending on the angle in friction. This relationship is as shown in equation 1

$$\begin{aligned} Q = \pi / 2dk_y \tan\theta\left(d_1{}^2 + L^2 + d_n{}^2\right) \\ +\pi / 4\left(B_1{}^2 - d^2\right)\left(1/2n\gamma B_1 N_\gamma + \gamma N_\gamma + N_q d_1\right). \end{aligned} \quad (1)$$

The effects of pull-out load on piles were further analyzed with the coexisting relations to the stress-strain relations [7]. This analysis was done in frozen sandy soils, and the stress-strain relationship proved to be linear. This approach was found to apply to the short pile only installed in moderately to densely over-consolidated clay soils hence a limiting factor in the predesign considering the fluctuating soil layers. The study further showed that during the loading process, the deformation of the earth along the pile perimeter acted similarly as the shearing of concentric cylinders hence the linearity in the stress and strain relations.

In the process of determining the pile failure mechanism, Kulhawy [8], came up with a general analytical model for the drained uplift capacity of drilled pile foundations. The main aim was to establish the main determining variables that will lead to the calculation of the ultimate loading capacity that produced the pile failure pattern. From his study, the uplift capacity, Q_u was a function of the foundation weight, W, pile tip resistance, Q_{tu}, pile side resistance, Q_{su}, length of the pile, D, and the shearing resistance along a general shear surface as shown in Figure 1.

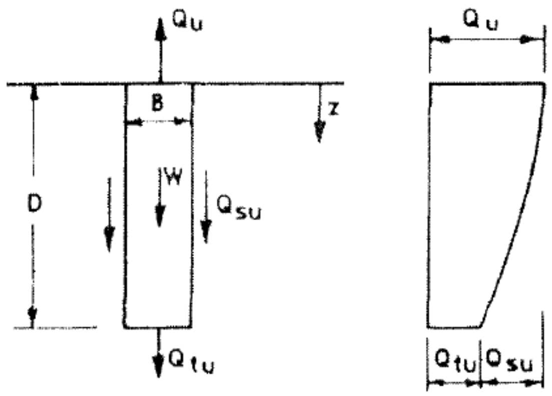

Figure 1. Uplift capacity function and the failure pattern by Kulhawy

Following these essential researches on the pile foundations, several experimental models have been developed to have an understanding of the pile-soil interaction during loading. These include the effects of repeated loading on the drained uplift capacity of the piles in granular soils [9] so as to examine the influence of the soil density and the pile diameter on the mechanism of the drilled shaft resistance, a study on the effects of straight piles and the piles with enlarged bases and roughness variation on the uplift capacity [10], and a study on the reaction of single piles embedded in layered sand under inclined pulling loads. The most recent researches have involved the development of scaled physical models [12], to study the responses of pile groups under uplift loads and an analytical method to predict the uplift capacity of the pile under study and, model tests on tabular steel tubes to analyze the effects of compressive load on the uplift capacity [13].

This study engages the use of numerical modelling to establish the foundation reaction concerning the uplift or pull-out loading. The numerical model uses the finite difference method embedded into the FLAC2D software to asses and computes the variation of the different input parameters, to obtain the desired output on pile performance. The reckoning is achieved mainly by the simulation of the stresses and the strains developed in the model grid during deformation by the applied corresponding velocities of the uplift load.

2. Modelling Technique

A numerical approach is a vital tool in the close examination of soil behavior under complex ground conditions. Most of the engineering problems associated with axial loading are always based on the axisymmetric point load solutions but FLAC2D is adapted to the plane-strain mode which is used to simulate equally spaces single piles. To obtain these critical results a finite element analysis mesh to replicate the real problem [14]is necessary as shown in Figure 2. The final model has been chosen so that the overall velocity field is distributed within the domain and no boundary effect is presented. In general, the model size has to be greater than 2 times the pile length (i.e. 2.8 m radius from pile element axis by 2.8 m depth).

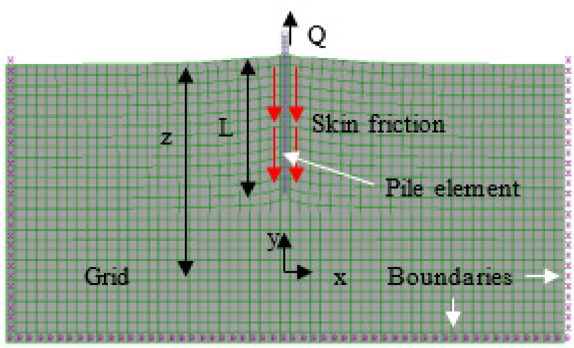

Figure 2. Generated mesh, boundary conditions and the pile element

This mesh places all the parameters to be input into the FLAC2D domain considering the pile and the soil interaction and the desired output.

The input parameters which include the soil properties and the pile element properties are as shown in Table 1 and Table 2 repectively.

Table 1. Soil Properties

Item	Type of soil			
	Silty soil	Clayey soil	Sandy soil	Units
Soil Density	1750	1750	2100	kg/m^3
Soil Cohesion	25e3	11e3	40e3	N/m^2
Soil Friction	30	0	22	Degree
Soil Dilatancy	15	0	15	Degree
Soil Tension	50e3	50e3	60e3	N/m^2
Young's Modulus	21e6	50e6	65e6	N/m^2
Poisons Ratio	0.3	0.3	0.35	Ratio

Table 2. Pile Element Properties

Item	Value	Units
Pile length below the ground surface	1.4	m
Pile diameter	0.26	m
Pile Young's modulus	8e10	N/m^2
Stiffness of shear coupling spring (**cs sstiff**)	1.3e11	N/m^2
Cohesive strength of the shear coupling spring (**cs scoh**)	5e5	N/m
Frictional resistance of the shear coupling spring (**cs sfric**)	20	Degree
Stiffness of normal coupling spring (**cs nstiff**)	1.3e8	N/m^2
Cohesive strength of the normal coupling spring (**cs ncoh**)	5e3	N/m
Frictional resistance of the normal coupling spring (**cs nfric**)	10	Degree

FLAC2D software then employs the Finite difference codes to provide a step by step integration of the input parameters for time and the set loading velocity. The products of the combination are summed up in the plane-strain mode which places the pile as a wall extending out of the plane of the cross-section (grid). FLAC2D, therefore, calculates the vertical stresses which area representative of the skin friction along the pile and the grid (soil) interface. These stress calculations are computed by the FISH function embedded in FLAC2D within all the zonal centroids in the model grid which is a representative of the soil component. Considering the forces represented in Figure 1, the calculated vertical stresses, σ_{yy} in the axial direction, can be described theoretically as shown in equation 2 for $y_y \geq z\text{-}L$ and equation 3 for $y_y \leq z\text{-}L$. Where y_y is the vertical displacement, z is the depth of the overburden soil layer, L is the length of the pile and x is the horizontal displacement

$$\sigma_{yy} = Q/\pi L\left(ln\frac{x^2}{(z-y)^2+x^2}+\frac{(z-y)^2}{(z-y)^2+x^2}\right) \quad (2)$$

$$\sigma_{yy} = Q/\pi L\left[\begin{array}{l} ln\dfrac{(z-L-y)^2+x^2}{(z-y)^2+x^2} \\ +\dfrac{x^2}{(z-L-y)^2+x^2}+\dfrac{x^2}{(z-y)^2+x^2}\end{array}\right]. \quad (3)$$

Ones all the input parameters and coded into the program, numerical stepping is therefore initiated, and the results obtained analyzed and plotted to capture the relationship between the axial/pull-out load and the vertical displacement. Also, the deformation of the grid/soil, the stress and strain concentrations and directions on the grid, bending moments on the pile and shear plane of failure as discussed in the next chapter.

3. Results and Discussion

In this paper, the finite difference numerical method is used to analyze the interaction of the pile element and the soil element. This analysis is done by the presentation of the corresponding pile head displacement curves during axial loading together with a comprehensive parametric study to show a particular design phenomenon. The analysis, therefore, helps engineers in project optimization while maintaining good foundation strength. Figure 3 represents the loading characteristics of the pile element under different grid mediums. The pile element is simulated in three types of soils namely, clay soils, silty soils and dense sandy soils. The pile head displacement curves show that sandy soils bear the most robust load handling capacity with maximum axial loads up to 94kN at minimal axial pile head displacements of 10mm. Silty soils and clay soils attain values of 90kN and 80kN respectively at 10mm axial pile head displacements.

FLAC2D provides a visual display of the soil movements during axial loading as shown in Figure 4. The deformations on the grid show a high upward movement of the overburden soil around the pile and grid interface and this movement reduces as the distance from the center of the pile element increases. This upward movement of the media is due to the vertical stress produced around the pile element due to the skin friction. In the process of axial loading, the load is transferred through the specified media by uniform skin friction hence the increment in axisymmetric deformation. This symmetry is shown in Figure 5 which represents the contour map of the effective stress on both sides of the pile elements. The stresses recorded in the grid range from -3E04 to 4E04 N with the intensities demarcated by the color coding, where light blue and red show the areas that experience maximum stresses and minimum stresses respectively.

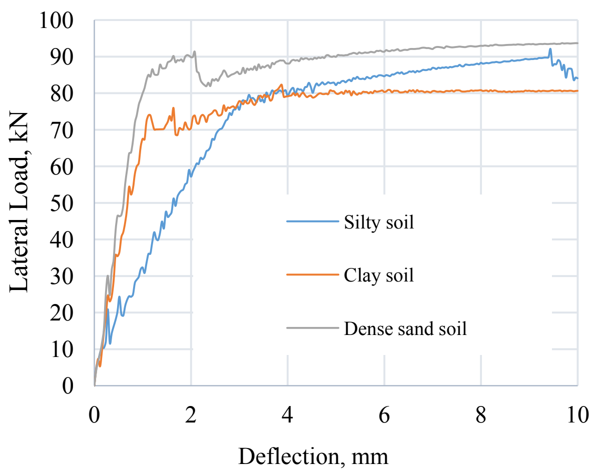

Figure 3. Pile head displacements at different axial loads

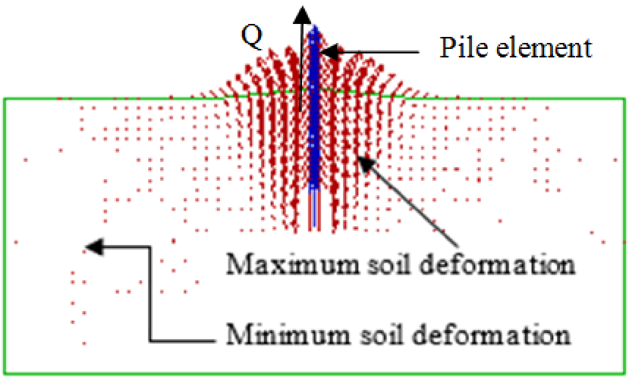

Figure 4. Ground movements during axial loading

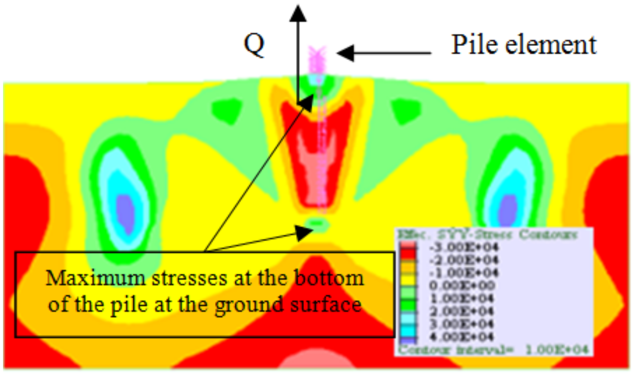

Figure 5. Contour zone for effective stress distribution on the grid

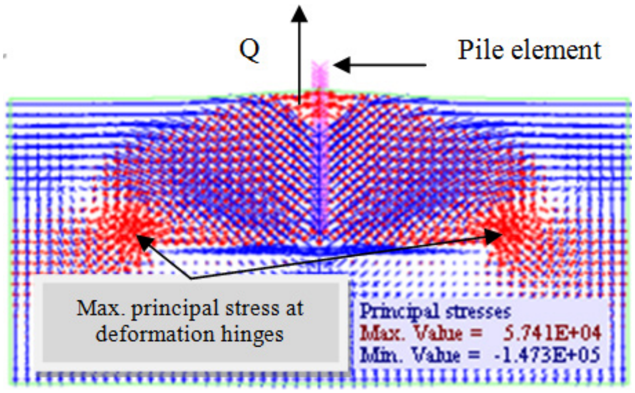

Figure 6. Effective Principal stress tensor distribution on axial loading

Figure 6 represents an in-depth view of the distribution of the principal stress tensors in the network during axial loading. It is evident that extreme stresses are felt around the pile/grid interface close to the ground surface and axisimmetrically deep into the grid at points that act as the hinges to the vacuum created due to the movement of the overburden weight. These high stresses are due to the high rates of grid deformations at these junctions as the pile element is pulled out. In theory, this behavior is represented by linear springs under the axial force that is dependent on the direction of the pile element movement, in this case along the y-axis.

To further understand the pile /grid interface, a contour view of the maximum shear strain shows the areas of high deformations as shown in Figure 7. The shear strain developed along the pile is also dependent on the cohesive strength of the pile/grid interface as well as the frictional resistance on the perimeter of the pile element. As the axial load is applied, the strain at the bottom of the pile increase up to 1.5e-1 which is recorded as the highest due to the high rates of deformations on the grid.

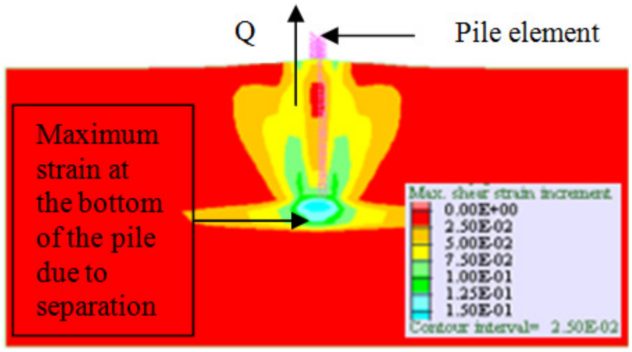

Figure 7. Maximum shear strain increment around the pile element

4. Parametric Study

4.1. Variation of the Pile Foundation Depth

The depth of the foundation is one of the major components that dictate the strength of the structure upon completion. This strength is due to the ability to transmit all the overburden load into the soil without any fear of structural failure. In this study, the depth of the foundation is varied in steps of 0.7m, 1.0m, 1.4m, 2.0m. From the FLAC2D output, it's evident that there is a linear relationship between the depth of the foundation and the ultimate axial load the pile can withstand before failure point. Considering the three types of soil involved in this model i.e. dense sand, silty soil and clay soil, dense sand has the highest permissible ultimate axial load of 130.22kN at 2.0m depth and the minimum allowable axial load of 38.54kN obtained from the clay soil at 0.7m depth as shown in Figure 8.

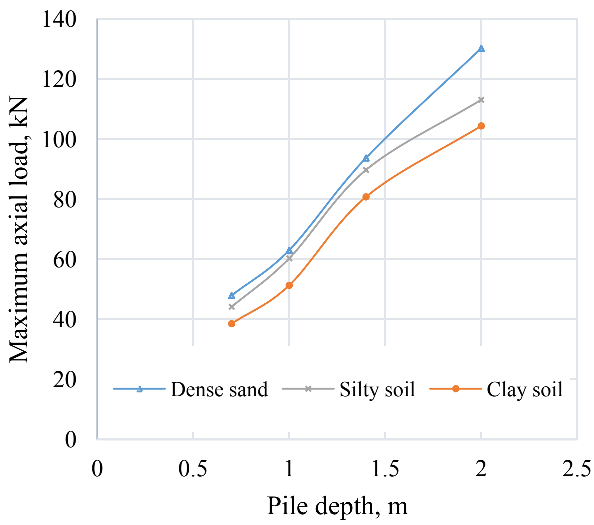

Figure 8. Variation of the foundation depth

4.2. Variation of the Angle of Internal Friction

The angle of internal friction is an essential parameter in the estimation of the ability of the soil to withstand the shear stresses experienced within the ground during loading. By replicating this into the input parameters of FLAC2D software, the effects of a range of the angle of internal friction gives a corresponding impact on the bearing capacity of the pile foundation. This angle is the angle measured between the normal force and the resultant force that is attained upon failure in response to the shearing stress. In this model, the angle of internal friction is analyzed at 10^0, 20^0, 30^0 and 40^0 for silty soil, dense sand and clay soils with increasing sand component. The plot shows a curvilinear relationship with maximum values recorded at the 20^0 angle in internal friction. The maximum values of the ultimate axial load obtained are 93.67kN and 85.78kN for dense sand and silty soils respectively. Sandy clay depicted a dramatic reduction in bearing capacity as the angle of internal friction increased to 40° where the ultimate axial load fell to 64.23kN as shown in Figure 9.

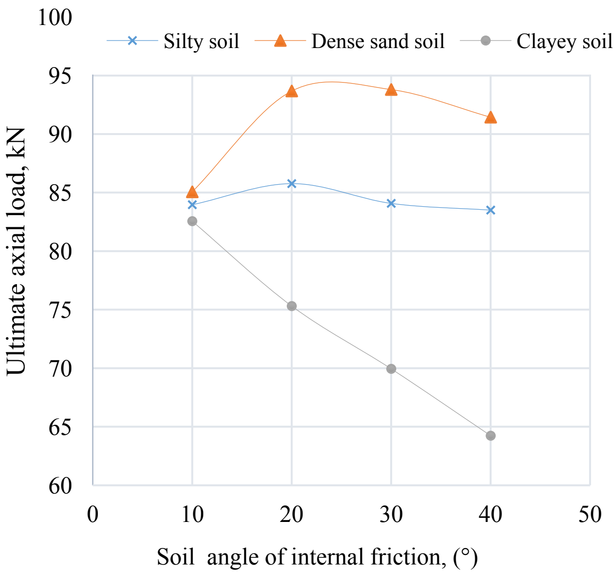

Figure 9. Influence of the angle of internal friction of the soil

4.3. Influence of Gap Formation during Loading

In this FLAC2D model, the interaction between the pile element and the grid can be represented by the normal and the shear coupling springs that tend to squeeze the grid/soil medium element on to the pile element. The pressing ensures a continuous wall/ medium contact. During the application of the axial load, this constant contact may be affected in a way that tends to bring in separation called the gap formation. The gap is mainly evident upon the failure of the structure itself from the ultimate load recorded. From this experiment, two formulations are taken into account that is, analysis with the expectation of gap formation and the other analysis without the gap formation. From the output, it is recorded that for sandy soil, and clay soil, the creation of gap has minimal effects on the ultimate load recorded and the differences in the pile head displacements. On the other hand, silty soils attain a higher final pressure when no gap formation is occurring than when there is no gap. The model with no gap and full gap predicts an ultimate load of 85kN and 80kN respectively as shown in Figure 10.

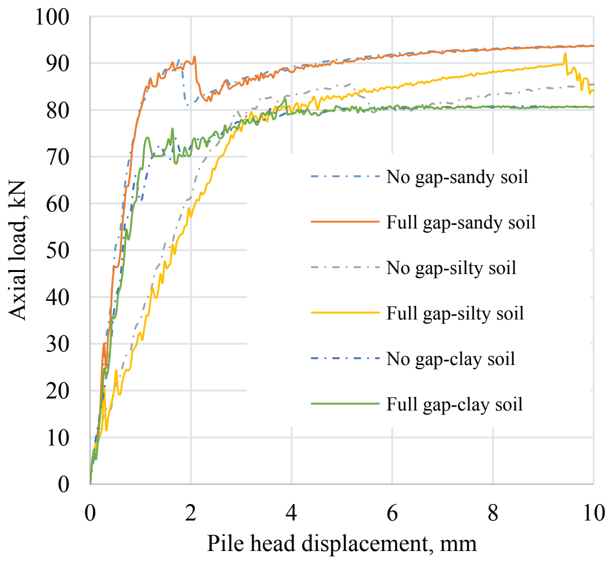

Figure 10. Effects of the gap on the ultimate axial load

5. Conclusion

This study focused on the analysis of the pile structural element for strength and the ability to resist the axial loads subjected to it. Axial loads are the forces that tend to pull the structure of the soil medium. Such effects are due to earthquakes or winds depending on the area of the basic installation. The approach used in this paper is the numerical simulation approach using FLAC2D which employed the use of finite difference method embedded within the program to determine the shear capacity of the pile during loading. The results are a clear indication of good strength with permissible loads shooting up to slightly above 90kN. The load can withstand external forces that may be subject to the pile foundation. In this study, the pile foundation is focused on supporting the solar panels at a cheaper cost than the existing structures. The aim is also based on the economics with more emphasis on the material costs for the realization of green energy in the developing countries. The parametric study further portrays an indication of the pile foundation flexibility for use in a variety of soil mediums with a minimum fluctuation of the strength properties. The result is vital in giving design engineers an in-depth understanding of the new foundation approach for proposed structural developments. Further research is necessary to determine the effects of the variable shape of the piles on the ultimate bearing capacity considering the structure to be constructed.

Acknowledgements

Thanks are also to Japan International Cooperation Agency (JICA) for giving the postgraduate scholarship to the first.

References

[1] Begemann, H.K.S., The Maximum Pulling Force on a Single Tension Pile Calculated on the Basis of Results of the Adhesion Jacket Cone, *Proc. 7th International Conference on SMFE*, 1965.

[2] Downs. D.L and Chieurzzi, R, *Transmission Tower Foundations*, Journal of Power Division, ASCE. Vol.92, No.2, 1966, pp. 91-114.

[3] Sowa, V.A., Pulling Capacity of Concrete Cast-In-Situ Bored Piles, *Canadian Geotechnical Journal*, Vol.7, 1970, pp. 482-493.

[4] Meyerhof, G.G., Uplift Resistance of Inclined Anchors and Piles, *Proceedings 8th International Conference on SMFE*, Moscow. Vol.2, 1973, pp. l67-173.

[5] McClelland, B., Design of Deep Penetration Piles for Ocean Structures, *Journal of GTE Division, ASCE*, Vol.100, 1974, pp.709-745.

[6] Sharma, B.V.R., *Uplift Capacity of Anchor Piles in sand Under Axial Pulling Loads,* M. Tech Thesis, 1988, Kharagpur, India.

[7] Poorooshasb, H.B., and Paramesw V.R., *Uplift of Rigid Piles in Frozen Sand*, Soils and Foundations, Vol.22, No.2, 1982, pp. 82-88.

[8] Kulhawy, F.H., Kozera, D.W., and Withium, J.L., Uplift Testing of Model Drilled shafts in Sand, *Journal of GTE Division, ASCE*. Vol. 105, 1979, pp. 31-47.

[9] Kulhawy, F.H., Drained Uplift Capacity of Drilled Shafts, *11th International Conference on SMFE*, San Francisco. Vol. 3, 1985, pp. l549-1551.

[10] Turner, J.P., and Kulhawy, F.H., Drained Uplift Capacity of Drilled Shafts Under Repeated Loading, *Journal of GTE Division*, Vol.116, 1990, pp. 470-491.

[11] Sharma, B.V. and Pise, P.J., *Uplift Capacity of Anchor Piles in Sand Under Axial-Pulling Loads*, IGJ, Vo1. 24, 1994, pp. 181-203.

[12] Patra, N.R. and Pise, P.J., Ultimate Lateral Resistance of Pile Groups in Sand, *Journal of Geotechnical and Geo-Environmental Engineering Division, ASCE*, Vol. 127, 2001, pp. 481-487.

[13] Das, B.K. and Pise, P.J., Effect of Compressive Load on Uplift Capacity of Model Piles, *Journal of Geotechnical and Geo-Environmental Engineering Division, ASCE*, 2003, Paper No.023132.

[14] Lysmer J., Limit analysis of plane problems in soil mechanics, ASCE *Journal of the Soil Mechanics and Foundations Division*, vol. 96, 1970, pp. 1311-34.

[15] Geddes, J.D., *Boussinesq-Based Approximations to the Vertical Stresses Caused by Pile-Type Subsurface Loadings*, Geotechnique V19(4), 1969, pp. 509-514.

[16] Cernica, J.N., Foundation Design, in Geotechnical Engineering. John Wiley, 1995.